Nucleon-Nucleon Correlations and Two-Nucleon Currents in Exclusive $(e, e'NN)$ Reactions

D. Knödler and H. Müther
Institut für Theoretische Physik, Universität Tübingen,
Auf der Morgenstelle 14, D-72076 Tübingen, Germany

P. Czerski
Instytut Fizyki Jadrowej, Pl-31-342 Krakow, Poland
(February 9, 2008)

The contributions of short-range nucleon-nucleon (NN) correlations, various meson exchange current (MEC) terms and the influence of Δ isobar excitations (isobaric currents, IC) on exclusive two-nucleon knockout reactions induced by electron scattering are investigated. The nuclear structure functions are evaluated for nuclear matter. Realistic NN interactions derived in the framework of One-Boson-Exchange model are employed to evaluate the effects of correlations and MEC in a consistent way. The correlations correlations are determined by solving the Bethe-Goldstone equation. This yields significant contributions to the structure functions W_L and W_T of the $(e, e'pn)$ and $(e, e'pp)$ reactions. These contributions compete with MEC corrections originating from the π and ρ exchange terms of the same interaction. Special attention is paid to the so-called 'super parallel' kinematics at momentum transfers which can be measured e.g. at MAMI in Mainz.

PACS numbers: 24.10.-i, 25.30.Rw, 21.65.+f

I. INTRODUCTION

It is well known that nuclei form a many-body system of interacting nucleons which exhibit strong correlations beyond the mean field or Hartree-Fock approximation. The strong short-range and tensor components of a realistic model for the nucleon-nucleon (NN) interaction induce corresponding two-body correlations. Many attempts have been made to explore the details of these correlations. Photoinduced exclusive two-nucleon knockout experiments like (γ, NN) or $(e, e'NN)$ reactions seem to be an ideal tool for such investigations as the cross section is related to the probability that the real or virtual photon is absorbed by a pair of interacting nucleons. The analysis of exclusive two-nucleon knockout experiments is restricted to such cases, in which momentum and energy conservation ensures that the residual nucleus with $A-2$ nucleons is produced in its groundstate or another well defined bound state. Due to the progress in accelerator and detector technology such triple coincidence experiments with good resolution have become possible and first results have been reported in the literature [1–3].

In studying such reactions, however, it is important to keep in mind that there exist various competing mechanisms which all contribute to the cross section of two-nucleon knockout. Beside the contribution which is due to the pair correlations in the ground state wavefunction one must consider the effects of the two-body terms in the operator for the electromagnetic current. These two-body terms include meson exchange currents (MEC) which can be derived from the commutator of the charge density with the nuclear Hamiltonian to obey the continuity equation. These meson exchange current contributions should be evaluated in a way consistent with the NN interaction used to describe the nuclear structure [4,5]. In the present work we investigate the MEC effects which are due to the exchange of π and ρ mesons.

In addition, there are contributions to the two-body current which are of a different origin. Here we, mention the contribution due to the excitation of intermediate Δ isobar excitations [9]. The contribution of this isobar current (IC) is not constrained by a continuity equation like the MEC and therefore depends on parameters like the meson-nucleon Δ coupling constants and the propagator of the Δ in the nuclear medium. The latter be chosen within certain limits.

Furthermore one should keep in mind that the so-called realistic NN interactions which we will employ in our study, like the Bonn potential [10], have been fitted to the NN scattering phase shifts at energies below the threshold for π productions. Therefore one should also restrict the analysis of $(e, e'NN)$ reactions to this regime.

The effects of two-body correlations have often been taken into account by assuming a local, state-independent correlation function between the interacting nucleons. From studies of single-nucleon knockout experiments, however, it is known that the energy dependence of the single-particle spectral function is essential for the understanding of the reaction mechanism [11,12]. Therefore, one would like to consider dynamical, state-dependent correlations in the

investigation of the two-body knockout, too. One way of achieving this goal is to evaluate the matrix elements for the photon absorption by a correlated pair of nucleons directly in terms of the Brueckner G matrix and the corresponding propagators for the nucleons.

In this manuscript we will describe a technique that allows to evaluate the nuclear matrix elements for the absorption of a photon by a correlated pair of nucleons, the MEC and the IC in a consistent scheme which includes the effects of the final state interaction of the outgoing nucleons with the residual nucleus in a mean field approximation. As a first step, this technique is applied to the absorption of the photons by nucleons in infinite nuclear matter. This allows to compare the relative importance of these different mechanisms and their interference under various kinematical conditions.

It is of course a serious disadvantage of such a study in nuclear matter that it does not provide results for a cross section which can directly be compared with experimental data produced for a specific target nucleus. In particular, it is impossible to take advantage of the fact that reactions leading to specific final states of the residual nucleus can be selective for one of the two-nucleon knockout mechanisms discussed above. Such a feature has been observed in theoretical studies of $(e,e'pp)$ an $(e,e'pn)$ reactions on ^{16}O [13,14]. On the other hand, however, a study of nuclear matter shall exhibit general features which are independent on the specific target nucleus considered and the corresponding long-range or low-energy correlations. A comparison of results for nuclear matter with those obtained for finite systems should enable us to disentangle effects which are global and due to the short-range behaviour of two nucleon correlations from those sensitive to surface and finite size effects. Furthermore such a study shall also allow to explore systematically the importance of e.g. the MEC originating from the ρ meson, which is often ignored. Finally, a study in nuclear matter shall also help to choose efficient setups for experiments which are selective in the sense that they yield results which are particularly sensitive to either the exploration of short-range correlations, MEC or IC contributions to the two-nucleon knockout reaction.

After this introduction we will present a description of the methods used to calculate the various contributions to the photoinduced two-nucleon knockout reactions in section 2. The detailed discussion of results is presented in section 3. Some concluding remarks are added in the final section 4.

II. THE CROSS SECTION AND THE NUCLEAR CURRENT

We start from the definition of the nine-fold differential cross section of the $(e,e'2N)$ reaction [15,16]

$$\frac{\mathrm{d}^9\sigma}{\mathrm{d}\tilde{E}_1\mathrm{d}\tilde{\Omega}_1\mathrm{d}\tilde{E}_2\mathrm{d}\tilde{\Omega}_2\mathrm{d}E'_e\mathrm{d}\Omega'_e} = \frac{1}{4}\,\frac{1}{(2\pi)^9}\,\tilde{p_1}\,\tilde{p_2}\,\tilde{E}_1\,\tilde{E}_2\,\sigma_{\mathrm{Mott}}\left\{v_C W_L + v_T W_T + v_S W_{TT} + v_I W_{LT}\right\} \times(2\pi)\,\delta(E_f - E_i) \tag{1}$$

where $\tilde{E}_1, \tilde{E}_2$ and $\tilde{p_1}, \tilde{p_2}$ denote the energies and momenta of the outgoing nucleons, respectively. The virtual photon created in the electron scattering process carries momentum $\vec{q}$ and energy ω. The leptonic structure functions v_i $(i = C,T,S,I)$ are defined by

$$\begin{aligned} v_C &= \left(\frac{q_\mu q^\mu}{\vec{q}^{\,2}}\right)^2 \\ v_T &= \tan^2\frac{\theta_e}{2} - \frac{1}{2}\left(\frac{q_\mu q^\mu}{\vec{q}^{\,2}}\right) \\ v_I &= \frac{q_\mu q^\mu}{\sqrt{2}|\vec{q}|^3}\,(E_e + E'_e)\,\tan\frac{\theta_e}{2} \\ v_S &= \frac{q_\mu q^\mu}{2\vec{q}^{\,2}} \end{aligned} \tag{2}$$

Here, θ_e is the angle of the scattered electron with respect to the incident electron beam and E_e, E'_e are the energies of the incident and the scattered electron, respectively.

The nuclear structure functions W_i $(i = L,T,TT,LT)$ contain the matrix elements of the nuclear current operator for a given photon polarization λ. These matrix elements are calculated for the current operator $\vec{J} = \vec{J}^{(1)} + \vec{J}^{(2)}$ which accounts for the different processes contributing to either the absorption of the photon energy and momentum on a single nucleon [cf. Figure 1, diagrams (a) and (b)] or on a pair of nucleons [cf. Figure 1(c) and the diagrams in Figures 2 and 3]. As a main aim of the investigation of the two-nucleon knockout reaction is to disentangle these different contributions all mechanisms have to be described with a consistent set of operators in order to avoid ambiguities

concerning e.g. coupling constants or cutoff masses. Within the framework of nuclear matter where the nucleons are described by plain-wave states we perform calculations for the different components of the nuclear current operator presented in detail in the following sections.

A. Ground-State Correlations and the Nuclear G Matrix

Figure 1 shows in diagram (a) and (b) the absorption of a photon carrying momentum $\vec{q}$ and energy ω on a single nucleon. This single nucleon is part of a correlated nucleon-nucleon pair. Here, correlations arising from the short-range and tensor components of the nucleon-nucleon interaction are calculated in terms of the nuclear G matrix [17]. As an example, we will discuss the evaluation of the diagram displayed in part (a) of Figure 1 using the notation displayed there. The matrix element which is required for the evaluation of the nuclear structure functions is calculated in a basis of plane-wave states

$$\int \mathrm{d}\vec{p}_a \, \langle \vec{p}_1{}' \,|\, H_{\gamma NN} \,|\, \vec{p}_a \rangle \, S(p_a, p_2') \, \langle \vec{p}_a \, \vec{p}_2{}' \,|\, G \,|\, \vec{p}_1 \, \vec{p}_2 \rangle. \tag{3}$$

Here and in the following, $\vec{p}_i$ denote the momenta of two uncorrelated nucleons in the target system. The center of mass momentum of this pair $\vec{P} = \vec{p}_1 + \vec{p}_2$ defines the total missing momentum of the two-nucleon knockout process. The single-particle energies referring to these momenta $\varepsilon_i = \varepsilon(p_i)$ will be parametrized in a simple effective mass approximation

$$\varepsilon(p) = \frac{p^2}{2m^*} + U \tag{4}$$

with an effective mass m^* and a potential U adjusted in such a way that (4) yields a good approximation for the single-particle energies evaluated in a Brueckner-Hartree-Fock calculation of nuclear matter [17]. The sum of the single-particle energies referring to the momenta $\vec{p}_i$ defines the total removal or missing energy $\varepsilon(p_1) + \varepsilon(p_2)$. The momenta $\vec{p}_1{}'$ and $\vec{p}_2{}'$ define the momenta of the outgoing nucleons inside nuclear matter. The directions of these momenta correspond to the direction of the momenta $\tilde{p}_i$ finally observed in the detector. The modulus of these vectors $\vec{p}_i'$ is determined in such a way that the single-particle energies of the nucleons inside nuclear matter, calculated according to (4) coincide with the free energies of the nucleons moving with momenta $\tilde{\vec{p}}_i$. In this way, we account for the retardation of the outgoing nucleons in the mean field of the remaining nucleus. The energy conservation can be expressed by

$$\varepsilon(p_1) + \varepsilon(p_2) + \omega = \varepsilon(p_1{}') + \varepsilon(p_2{}') = \frac{\tilde{p_1}^2}{2m_N} + \frac{\tilde{p_2}^2}{2m_N} \,, \tag{5}$$

while the conservation of total momentum yields

$$\vec{p}_1 + \vec{p}_2 + \vec{q} = \vec{p}_a + \vec{p}_2{}' + \vec{q} = \vec{p}_1{}' + \vec{p}_2{}' \,. \tag{6}$$

The momentum $\vec{p}_a$ in (3) and (6) denotes the momentum of the intermediate single-nucleon state before the absorption of the photon (see also part (a) of Figure 1). The propagation of the intermediate two-nucleon state is described in terms of the propagator

$$S(p_a, p_2') = \frac{\mathcal{Q}(p_a, p_2')}{\varepsilon(p_1) + \varepsilon(p_2) - \varepsilon(p_a) - \varepsilon(p_2') + \mathrm{i}\eta} \tag{7}$$

with a Pauli operator $\mathcal{Q}(p_a, p_2')$ which ensures that the nucleons are propagating in states above the Fermi sea.

The absorption of the real or virtual photon carrying momentum $\vec{q}$ by the single (off-shell) nucleon with initial momentum $\vec{p}_a$ and final momentum $\vec{p}_1{}'$ is described by the Hamiltonian

$$H_{\gamma NN} = i\, e \, \frac{\mu_N}{2m_N} (\vec{\sigma} \times \vec{q}) \cdot \vec{\varepsilon} + e \, \frac{\delta_N}{2m_N} (\vec{p}_a + \vec{p}_1{}') \cdot \vec{\varepsilon} \tag{8}$$

where $\delta_N = 1$ for a proton and $\delta_N = 0$ for a neutron [18]. The vector $\vec{\varepsilon}$ refers to the polarization of the absorbed photon. Note that we employ here the non-relativistic reduction of the one-body current ignoring possible off-shell effects, which are due to a possible medium modification of the nucleons in the nuclear medium [19].

As the final ingredient, the nuclear G matrix has to be calculated. For a realistic nucleon-nucleon interaction described by a potential V, the Bethe-Goldstone equation

$$G = V + V \frac{\mathcal{Q}}{W - H_0 + \mathrm{i}\eta} G \tag{9}$$

has to be solved. Again the operator $\mathcal{Q}$ ensures that the Pauli principle is obeyed in the nuclear medium. The starting energy W is the sum of the single-particle energies $\epsilon(p_1) + \epsilon(p_2)$. The nuclear G matrix conserves the center of mass momentum of the interacting pair of nucleons $\vec{p}_1 + \vec{p}_2 = \vec{p}_a + \vec{p}_2{}'$ but leads to a redistribution of relative momenta between the two nucleons going up to several hundred MeV/c. The calculation of these G matrix elements is performed in a partial wave basis using the BONN A potential [10]. Also the effective masses m^* and values of the single-particle potential U are determined for this potential.

B. Meson Exchange Currents

Meson exchange currents (MEC) represent another possibility of absorbing a photon on a pair of nucleons. In this case, the real or virtual photon is absorbed in coincidence with the exchange of a virtual meson (π, ρ, σ, ω, ...) between the nucleon-nucleon pair. The corresponding current operators can be derived either by minimal coupling or via the continuity equation using meson exchange potentials [4,5].

Starting with a single-particle charge density $\rho = \frac{1}{2}\, e \sum_{i=1}^{A} (1 + \tau_{i,z})\, \delta(\vec{r} - \vec{r}_i)$ and inserting as an example the non-relativistic reduction of the π-exchange potential

$$V_{\pi NN} = -v_\pi(k)\, (\vec{\sigma}_1 \cdot \vec{k})\, (\vec{\sigma}_2 \cdot \vec{k})\, (\vec{\tau}_1 \cdot \vec{\tau}_2) \tag{10}$$

with $v_\pi(k) = \frac{f^2_{\pi NN}}{m^2_\pi} \frac{1}{m^2_\pi + k^2}$ in the continuity equation

$$\vec{\nabla} \cdot \vec{j} + i \left[H\, ,\, \rho \right] = 0 \tag{11}$$

yields the corresponding MEC operator

$$\begin{aligned} \vec{j}_\pi(\vec{k}_1, \vec{k}_2) = -i\, e\, \frac{f^2_{\pi NN}}{m^2_\pi}\, (\vec{\tau}_1 \times \vec{\tau}_2)_z \\ \times \left[\frac{\vec{\sigma}_1\, (\vec{\sigma}_2 \cdot \vec{k}_2)}{m^2_\pi + k^2_2} - \frac{\vec{\sigma}_2\, (\vec{\sigma}_1 \cdot \vec{k}_1)}{m^2_\pi + k^2_1} - \frac{(\vec{\sigma}_1 \cdot \vec{k}_1)(\vec{\sigma}_2 \cdot \vec{k}_2)}{(m^2_\pi + k^2_1)(m^2_\pi + k^2_2)} (\vec{k}_1 - \vec{k}_2) \right], \end{aligned} \tag{12}$$

which can be split into the so-called seagull [first two terms, cf. diagrams (a) and (b) of Figure 2] and pion-in-flight [cf. diagram (c) of Figure 2] terms. The isospin structure of this current operator yields a non-vanishing contribution only for the exchange of charged pions and therefore it will contribute to the knockout of a proton-neutron pair only.

In order to regularize the π-exchange potential at large momentum transfers k, the meson-nucleon vertices are multiplied by monopole type form factors

$$F(q) = \frac{\Lambda^2_\pi - m^2_\pi}{\Lambda^2_\pi + k^2} \tag{13}$$

This regularization must be taken into account before deriving the MEC operators to ensure that the continuity equation is satisfied up to second order in the nucleon-nucleon interaction.

In the same manner, the MEC operators corresponding to the exchange of a ρ meson can be derived [4,6]. For the case of two-nucleon knock-out it has been observed, however, that the effects of the ρ MEC corrections are not of particular significance [7] and could be simulated the cut-off parameter for the pion [8]. Therefore we do not include the effects of ρ MEC in the present investigation.

Another type of MEC operators is usually quoted as 'model dependent' in the sense that it cannot be deduced using the continuity equation. These operators either refer to the absorption of the photon on two different mesons [Figure 2(d)] or to processes involving the excitation or de-excitation of an intermediate Δ resonance (depicted in Figure 3).

To calculate the matrix elements of the current operator $\vec{j}_\pi(\vec{k}_1, \vec{k}_2)$, we refer to the kinematical setting described in the previous section. The momentum transfers $\vec{k}_1$ and $\vec{k}_2$ can then be determined via

$$\vec{k}_1 = \vec{p}_1{}' - \vec{p}_1 \quad and \quad \vec{k}_2 = \vec{p}_2{}' - \vec{p}_2. \tag{14}$$

Finally, the matrix element for the exchange of a π-meson in a plane-wave basis can be written as

$$\langle \vec{p}_1{}'\, \vec{p}_2{}' \,|\, \vec{j}_\pi(\vec{k}_1, \vec{k}_2) \,|\, \vec{p}_1\, \vec{p}_2 \rangle. \tag{15}$$

C. Isobaric Currents

Considering the inclusion of an intermediate Δ resonance leeds to two different reaction processes. Either the absorbed photon creates a Δ resonance which afterwards leads to the exchange of a charged or uncharged meson [cf. Figures 3 (a) and (b)] or the excitation of an intermediate Δ resonance is caused by the exchange of a meson and the final photon absorption is responsible for the de-excitation of the resonance [cf. Figure 3 (c) and (d)].

The construction of the corresponding operators is not possible via the insertion of a nucleon-nucleon potential in the continuity equation. In contrast to the deduction of the MEC operators in the previous section, here the operators for the isobaric currents are constructed by simply considering the three different components of the absorption process. According to [9], diagram (a) in Figure 3 may be described by the operator

$$\vec{j}_{\Delta}^{(a)} = -\frac{\mathrm{i}}{9}\,\frac{f_{\pi NN} f_{\pi N\Delta} f_{\gamma N\Delta}}{m_\pi^3}\,S_{\Delta}^{(a)}\,\frac{\vec{\sigma}_2\cdot\vec{k}}{m_\pi^2+\vec{k}^2}\left\{4(\vec{\tau}_2)_z\,\vec{k}+(\vec{\tau}_1\times\vec{\tau}_2)_z\,(\vec{k}\times\vec{\sigma}_1)\right\}\times\vec{q}, \tag{16}$$

which besides the momentum, spin, and isospin structure contains a propagator S_Δ for the intermediate Δ resonance. Transverse by construction, this operator satisfies the continuity equation and cannot contribute to $(e,e'2N)$ reactions with purely longitudinally polarized photons. In contrast to the MECs derived using the continuity equation, isobaric currents also allow for the exchange of uncharged mesons. They therefore contribute to the knockout of proton-proton pairs.

Similar to the outlined procedure, the derivation of the current operators for the three remaining diagrams in Figure 3 may be performed. Of course, the excitation of a Δ resonance by the absorption of a photon [diagrams (a) and (b)] requires a structure of the Δ propagator different from the propagators for diagrams (c) and (d). The calculation of S_Δ is performed according to [9] considering the invariant energy of the final two-nucleon state or the binding energies for the initial states plus the photon energy ω [see (5)]. Following this procedure, one gets for diagram (a) of Figure 3

$$S_\Delta = \frac{1}{\varepsilon(p_1)+\omega-\varepsilon_\Delta+\frac{\mathrm{i}}{2}\Gamma_\Delta(\omega)} \tag{17}$$

where $\varepsilon_\Delta = \frac{(\vec{p}_1+\vec{q})^2}{2m_\Delta}+m_\Delta-m_N$ is the energy of the Δ state with momentum $\vec{p}_1+\vec{q}$ including the ΔN mass difference. The Delta resonance is also given a decay width $\Gamma_\Delta(\omega)$ which shows a variation depending on the energy of the absorbed photon. For photon energies ω below 300 MeV we chose an energy dependent width according to [20]

$$\Gamma_\Delta(\omega) = \frac{8f_{\pi NN}^2}{12\pi}\,\frac{(\omega^2-m_\pi^2)^{\frac{3}{2}}}{m_\pi^2}\,\frac{m_\Delta-m_N}{\omega}. \tag{18}$$

Approximations which have often been used for the Δ propapgator include e.g. [26]

$$S_\Delta^{approx.} = \frac{1}{m_\Delta-m_N-\omega-\frac{\mathrm{i}}{2}\Gamma_\Delta(\omega)} \tag{19}$$

or even the static propagator

$$S_\Delta^{static} = \frac{1}{m_\Delta-m_N}. \tag{20}$$

In our calculations all nucleon-meson and Δ-meson vertices are multiplied by a monopole type form factor with the same cutoff mass Λ_π as in the previous section.

III. RESULTS AND DISCUSSION

All calculations are performed in nuclear matter at saturation density ($k_F = 1.35\,\mathrm{fm}^{-1}$). The coupling constants for the π exchange are $f_{\pi NN} = 1.005$, $f_{\pi N\Delta} = 2f_{\pi NN}$, and $f_{\gamma N\Delta} = 0.12$. We used a cutoff mass for the π-nucleon form factor of $\Lambda_\pi = 1.3\,\mathrm{GeV}$. In all considered cases, the MEC contributions contain the seagull and in-flight currents for the exchange of a π meson. Additional MEC contributions like the photon absorption on a pair of π and ρ mesons were found to give negligible contributions in all kinematical setups we investigated. The π-nucleon vertex is compatible with the π exchange part of the One-Boson-Exchange potential BONN A [10] we used to determine the G matrix for calculating the effects of NN correlations. The same potential has also been used to determine the single-particle

energies for the nucleons in the nuclear medium which were parametrized according to (4) by $m^* = 623\,\mathrm{MeV}$ and $U = -86.8\,\mathrm{MeV}$.

As a first example, we would like to consider the case of $(e, e'pp)$ reactions in the so-called 'super parallel' kinematical situation where the momentum $\vec{p}_1{}'$ of one knocked-out proton has the same direction as the photon momentum. The momentum of the second proton $\vec{p}_2{}'$ is opposite to this direction. The photon energy is fixed at $\omega = 215\,\mathrm{MeV}$. Results are shown in Figure 4. The left section of this figure displays results selecting an asymmetric distribution of the photon energy to the two protons. The one with final momentum parallel to $\vec{q}$ is chosen to have a final kinetic energy of $T_{p,1} = 156\,\mathrm{MeV}$ while the second one with momentum antiparallel to $\vec{q}$ has a final energy of $T_{p,2} = 33\,\mathrm{MeV}$. For comparison, we also present the example in which the photon energy is distributed in a more symmetric way with $T_{p,1} = 116\,\mathrm{MeV}$ and $T_{p,2} = 73\,\mathrm{MeV}$ in the right part of Figure 4. The upper part of this figure exhibits results for the longitudinal structure function W_L while the transverse structure function W_T is displayed in the lower parts of the figure.

As it has been discussed in the previous section, the MEC originating from π exchange do not contribute to the photon induced two-proton knockout process. The isobar currents (IC) only affect the transverse structure function W_T. Therefore, the results for the longitudinal structure functions W_L displayed in the upper part of Figure 4 are solely due to the effects of correlations. We can see that this correlation contribution W_L is significantly larger in the case of asymmetric energy distribution (upper left part of the figure) than in the case of more symmetric energy distribution. Note the different scales on these parts of the figures. The correlation contribution 'prefers' processes in which the momentum and the energy of the virtual photon is absorbed by one proton which is knocked-out parallel to the momentum $\vec{q}$, while the second proton receives only a smaller fraction.

The situation is rather similar for the transverse structure function W_T. Also here, the cross section due to correlations (dashed line) is significantly larger in the case of asymmetric energy distribution. The contribution of the IC to the structure function (dashed-dotted lines) is similar in magnitude for the two cases considered. The correlation and isobar contributions to the total structure function W_T (solid lines) are of similar importance for the more symmetric distribution of energy, while the correlation contribution is dominating the cross section in the asymmetric case, in particular at larger photon momenta.

As a next example, we discuss the $(e, e'pn)$ reaction under the same kinematical conditions. Here, we consider the case with the proton emitted parallel to the photon momentum and the neutron momentum antiparallel to $\vec{q}$. In this case, we have to take into account the effects of MEC as well (solid line with squares). Comparing the knockout of a proton-neutron pair to the ejection of a pair of protons, one observes that the structure functions for the $(e, e'pn)$ reaction are roughly 10 times bigger than the structure functions for the $(e, e'pp)$ reactions (see Figure 5). This fraction is slightly larger for transverse photon polarisation than for longitudinally polarized virtual photons. This enhancement of the structure functions is, of course, partly due to the MEC. We find, however, that the contribution of correlations to the structure functions alone are enhanced by roughly a factor of 7 comparing $(e, e'pn)$ with $(e, e'pp)$. This demonstrates the importance of tensor correlations which are more effective in the pn than in the pp interaction. We would like to recall that we have used the potential BONN A for the NN interaction. This interaction exhibits a rather weak tensor component as compared to other models for a realistic NN interaction. A measure for the strength of this tensor component is given by the D-state probability in the deuteron wavefunction. The BONN A potential yields a D-state probability of only 4.38 percent, while other meson exchange potentials predict D-state probabilities up to 6 percent [10]. Again, we notice that the correlation effect is stronger when the photon energy and momentum is distributed in a rather asymmetric way to the knocked-out nucleons (left column of Figure 5).

In the 'super parallel' kinematical setup, the MEC contribution is of particular importance in the transverse structure function (lower sections of Figure 5). It dominates the corresponding cross section in the case of the more symmetric energy distribution. In the asymmetric case, however, the ratio of MEC to correlation contribution depends in quite a sensitive way on the photon momenta and is in the average twice as large as the correlation contribution for the cases considered. The IC contribution is small in all these cases since the photon energy considered ($\omega = 215$ MeV) is below the threshold of the Δ.

In order to investigate the dependence of the MEC contribution on the kind of structure function, we display in Figure 6 the contribution of the π-seagull terms [diagrams (a) and (b) of Fig. 2] and the π-in-flight term [Fig. 2 (c)] separately for the asymmetric kinematic discussed in Figure 5. These contributions are of similar importance in the longitudinal structure function but cancel each other almost completely. Such a strong cancellation does not occur in the transverse channel in which the π-in-flight term dominates. Therefore, one may consider the longitudinal structure function for $(e, e'pn)$ reactions in 'super parallel' kinematics as an ideal setup to study effects of correlations.

A large contribution from MEC is observed in other kinematical setups. As an example, we show in Figure 7 the longitudinal and transverse structure functions depending on the photon momentum $|\vec{q}|$ for a symmetric splitting of the kinetic energies and the angles with respect to the direction of the momentum transfer of the outgoing particles ($T_p = T_n = 70\,\mathrm{MeV}$ and $\theta'_p = \theta'_n = 30^\mathrm{o}$). The photon energy was chosen to be $\omega = 230\,\mathrm{MeV}$. In this framework, the influence of the single-particle current (correlations) is almost negligible compared to the dominating MEC contribution. At

higher photon momenta, the isobaric current contribution gets even more important than the correlation contribution.

Finally, we would like to add a few remarks on the evaluation of the isobar contribution to the two-body current. As an example, we consider in Figure 8 the IC contribution to the transverse structure function of $(e, e'pn)$ using the kinematical setup of Figure 5 (left part). The IC contribution is rather sensitive to the approximation employed for the Δ propagator [22,23]. The correct evaluation of the propagator (17) for the resonant [Figure 3 (a) and (b)] and non-resonant [Figure 3 (c) and (d)] terms, as discussed above, leads to an IC contribution (solid line) which is significantly smaller than the one obtained if a propagator of the form (19) is used for the resonant as well as the non-resonant case (dashed line). The static propagator (20) replacing the energy denominators for the propagators in all four terms of the Figure 3 by the Δ nucleon mass difference leads to a structure function (dashed-dotted line) which is roughly a factor of three larger than the exact result and also the propagator suggested in [24] (dotted line) overestimates the correct result by roughly a factor of two.

IV. SUMMARY AND CONCLUSIONS

The contributions originating from nucleon-nucleon correlations, meson-exchange currents (MEC) and isobar currents (IC) to the cross section for photon induced two-nucleon knock-out reactions $(e, e'2N)$ have been investigated by evaluating the corresponding matrix elements in a consistent way for a system of infinite nuclear matter. The relative importance of these various contributions is quite sensitive to the kinematical setup of such triple coincidence experiments. The so called super-parallel kinematic turns out to be very appropriate for the investigation of NN correlation effects. This is particularly true for reactions in which momentum and energy of the absorbed photon are transfered predominantly on one of the nucleons knocked-out: Correlations seem not to be very 'efficient' to transfer large amounts of energy to the second nucleon.

The $(e, e'pp)$ reactions are favourable for the study of NN correlations because the competing two-body current contributions are suppressed: The MEC from π-exchange which dominate $(e, e'pn)$ reactions don't contribute in this case and IC only show up in the transverse structure function. However, it is very important to investigate $(e, e'pn)$ reactions as well. The pn correlations are quite different from the pp correlations, the structure functions originating from correlation effects are by a factor of 5 to 10 larger for the pn knock-out than for $(e, e'pp)$.

The MEC contributions which are dominating in many kinematical setups, are highly suppressed in the 'super parallel' kinematics in which the proton is observed in the direction of the photon and the neutron is detected anti-parallel to the momentum of the photon. The suppression of the MEC is due to a strong cancellation between the π-seagull and π-in-flight contribution. The correlation effects should show up in particular in the longitudinal structure function in this kinematical setup.

The present study includes the effects of a final state interaction between the knocked-out nucleons and the residual interaction on the level of a mean-field approximation. One should also consider, however, the contribution to the cross section which originates from the direct interaction of the two nucleons after the absorption of the photon. This can be done in the scheme outlined in this manuscript. The importance of the final state interaction has been demonstrated e.g. in the Monte-Carlo simulations of ref. [27]. The consistent calculation scheme for correlations, two-body currents and final state interaction should also be applied directly to the evaluation of cross section for specific target nuclei.

The authors wish to thank Peter Grabmayr for fruitful discussions. This research project has partially been supported by the SFB 382 of the Deutsche Forschungsgemeinschaft and the DFG-Graduiertenkolleg GRK 132.

---

[1] K. I. Blomqvist *et al.*, *Phys. Lett.* **B421** (1998) 71.
[2] C. J. G. Onderwater *et al.*, *Phys. Rev. Lett.* **81** (1998) 2213.
[3] G. Rosner, Proc. on "Perspectives in Hadron Physics", eds. S. Boffi, C. Cioffi degli Atti and M. Giannini, p. 185 (World Scientific 1998).
[4] J.-F. Mathiot, *Phys. Rep.* **173** (1989) 64.
[5] D. O. Riska, *Phys. Rep.* **181** (1989) 208.
[6] I.S. Towner, *Phys. Rep.* **155** (1987) 263.
[7] M. Vanderhaeghen, L. Machenil, J. Ryckebusch, and M. Waroquier, *Nucl. Phys. A* **580** (1994) 551.
[8] L. Machenil, M. Vanderhaeghen,. Ryckebusch, and M. Waroquier, *Phys. Lett. B* **316** (1993) 17.
[9] P. Wilhelm, H. Arenhövel, C. Giusti, and F. D. Pacati, *Z. Phys. A* **359** (1997) 467.

[10] R. Machleidt, *Adv. Nucl. Phys.* **19** (1989) 189.
[11] H. Müther, A. Polls, and W. H. Dickhoff, *Phys. Rev. C* **51** (1995) 3040.
[12] K. Amir-Azimi-Nili, J. M. Udias, H. Müther, L. D. Skouras, and A. Polls, *Nucl. Phys. A* **625** (1997) 633.
[13] C. Giusti, F. D. Pacati, K. Allaart, W. J. W. Geurts, W. H. Dickhoff, and H. Müther, *Phys. Rev. C* **57** (1998) 1691.
[14] C. Giusti, H. M"uther, F. D. Pacati, and M. Stauf, preprint nucl-th/9903065.
[15] C. Giusti and F. D. Pacati, *Nucl. Phys. A* **535** (1991) 573.
[16] J. Ryckebusch, M. Vanderhaeghen, K. Heyde, and M. Waroquier, *Phys. Lett. B* **350** (1995) 1
[17] H. Müther and P. U. Sauer, in *Computational Nuclear Physics 2*, edited by K. Langanke, J. A. Maruhn and S. E. Koonin, Springer, New York (1993).
[18] T. Ericson and W. Weise, *Pions and Nuclei*, Oxford University Press (1988).
[19] S. Boffi, C. Giusti, F.D. Pacati and M. Radici, *Electromagnetic Response of Atomic Nuclei*, Clarendon Press, Oxford (1996).
[20] E. Oset, H. Toki, and W. Weise, *Phys. Lett. B* **83** (1982) 281.
[21] P. Grabmayr et al., Proposal Mainz Microtron MAMI "First Study of the ^{16}O$(e,e'np)^{14}$N Reaction", A1/5-98 (Spokesperson: R. Neuhausen).
[22] T. Wilbois, P. Wilhelm, and H. Arenhövel *Phys. Rev. C* **54** (1996) 3311.
[23] J. Ryckebusch, L. Machenil, M. Vanderhaeghen, V. Van der Sluys, and M. Waroquier, *Phys. Rev. C* **54** (1996) 3313.
[24] J. Ryckebusch, V. Van der Sluys, K. Heyde, H. Holvoet, W. Van Nespen, and M. Waroquier, *Nucl. Phys.* **A624** (1997) 581.
[25] J. Ryckebusch, M. Vanderhaeghen, L. Machenil, and M. Waroquier, *Nucl. Phys.* **A568** (1994) 828.
[26] J. Ryckebusch, L. Machenil, M. Vanderhaeghen, V. Van der Sluys, and M. Waroquier, *Phys. Rev. C* **49** (1994) 2704.
[27] A. Gil, J. Nieves, and E. Oset, *Nucl. Phys.* **A627** (1997) 599.

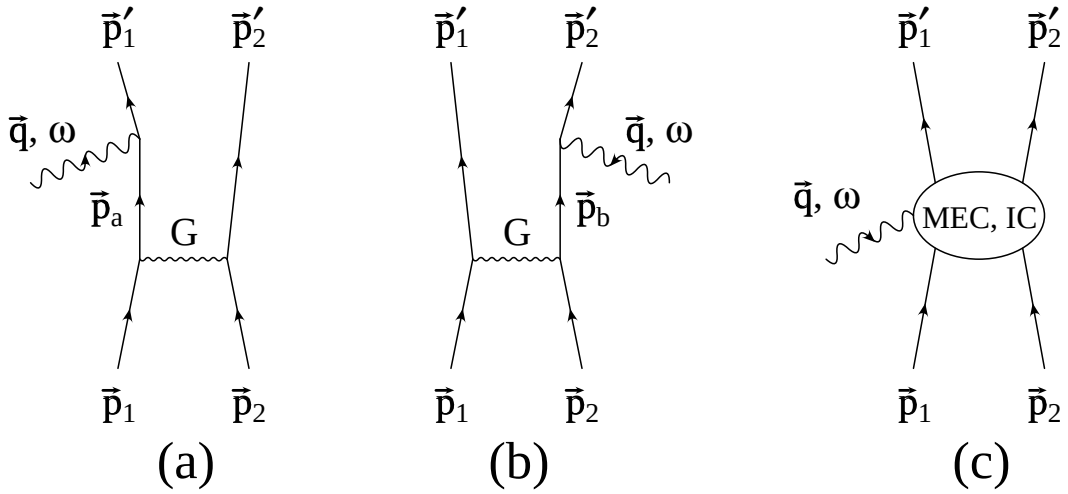

FIG. 1. Diagrams for the different processes contributing to the $(e,e'2N)$ reaction. Diagram (a) and (b) show the absorption of the photon by a single nucleon. The nucleon-nucleon correlations are described by the G matrix. Diagram (c) depicts photon absorption via meson exchange (MEC) or isobaric currents (IC) (cf. Figures 2 and 3).

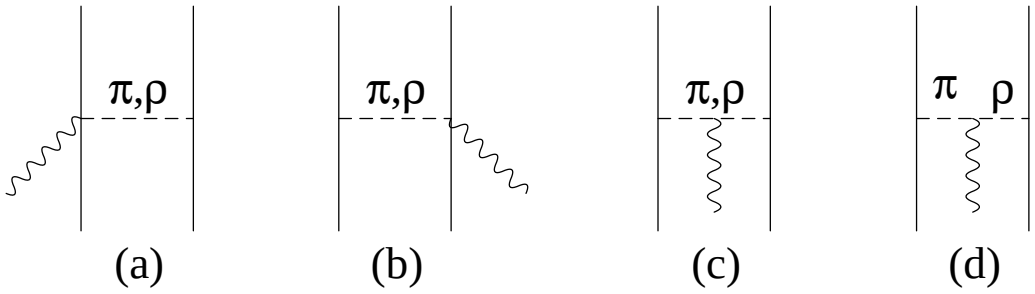

FIG. 2. MEC operators: Diagrams (a) and (b) show the seagull term for the exchange of a π or a ρ meson respectively, diagram (c) shows the meson-in-flight contribution, and (d) illustrates the coupling of the photon to a π and a ρ meson.

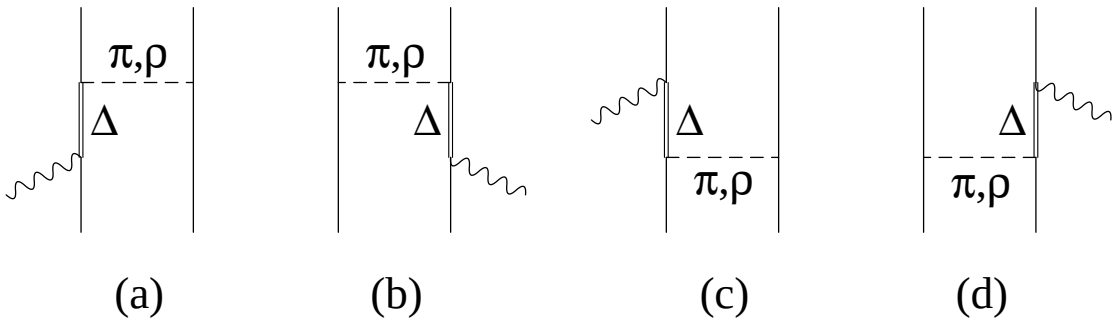

FIG. 3. Isobaric current contributions. Diagrams (a) and (b) show the excitation of the Δ resonance due to the absorption of a photon. The intermediate resonance is de-excited by the exchange of a π or a ρ meson. In diagrams (c) and (d) meson exchange creates a Δ resonance which is de-excited by the absorption of a photon.

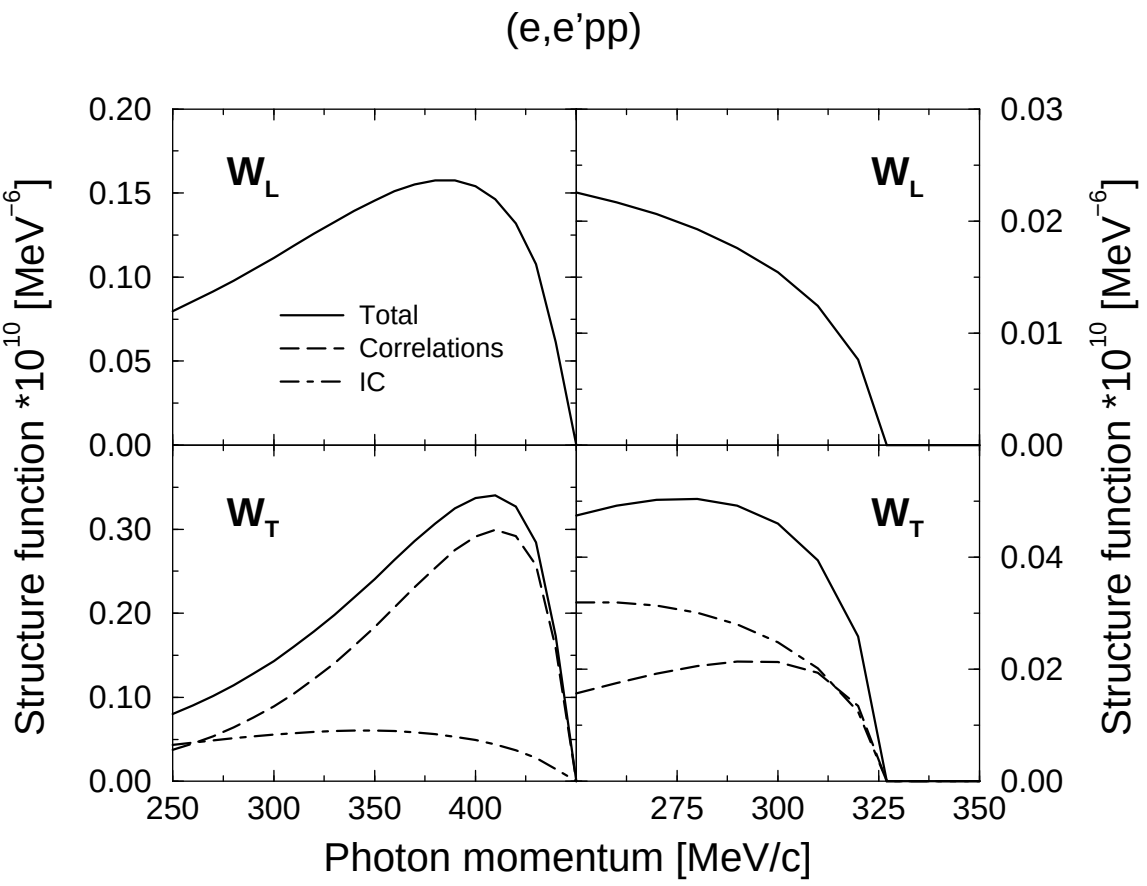

FIG. 4. Longitudinal (upper part) and transverse structure functions (lower part) for the knockout of a proton-proton pair in a 'super parallel' kinematical situation with angles $\theta'_{p,1} = 0^{\circ}$ and $\theta'_{p,2} = 180^{\circ}$ of the two protons with respect to the direction of the photon momentum. The left part of the figure assumes final kinetic energies $T_{p,1} = 156\,\mathrm{MeV}$ and $T_{p,2} = 33\,\mathrm{MeV}$ of the two protons while in the right part the final kinetic energies are $T_{p,1} = 116\,\mathrm{MeV}$ and $T_{p,2} = 73\,\mathrm{MeV}$. The photon energy was chosen to be $\omega = 215\,\mathrm{MeV}$ in all cases. Together with the total structure functions (solid line) the contributions arising from correlations (dashed line) and IC (dot-dashed line) are shown. Please note the different scales.

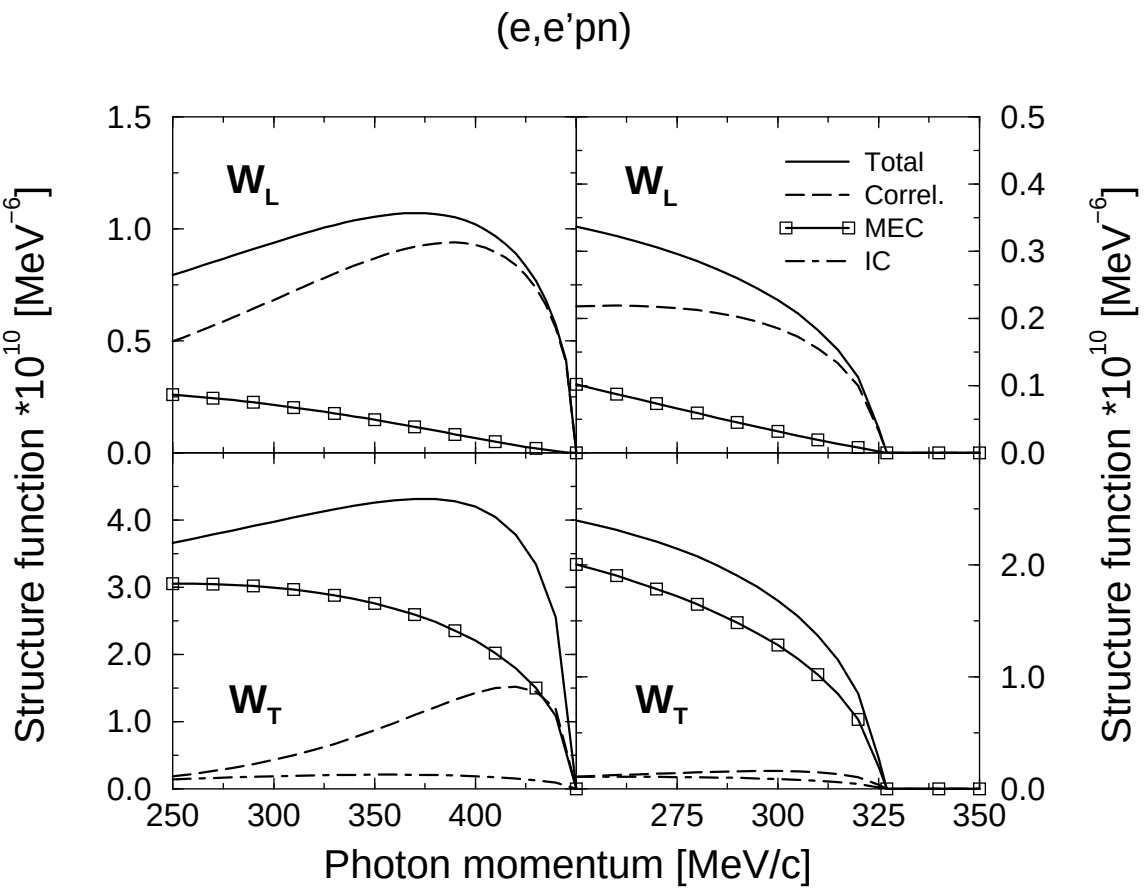

FIG. 5. Longitudinal (upper part) and transverse structure functions (lower part) for the knockout of a proton-neutron pair in a 'super parallel' kinematical situation with angles $\theta'_p = 0^\circ$ and $\theta'_n = 180^\circ$ of the proton and the neutron with respect to the direction of the photon momentum. The left part of the figure assumes final kinetic energies $T_p = 156\,\mathrm{MeV}$ and $T_n = 33\,\mathrm{MeV}$ of the two protons while in the right part the final kinetic energies are $T_p = 116\,\mathrm{MeV}$ and $T_n = 73\,\mathrm{MeV}$. The photon energy was chosen to be $\omega = 215\,\mathrm{MeV}$ in all cases. Together with the total structure functions (solid line) the contributions arising from correlations (dashed line), MEC (solid line with squares) and IC (dot-dashed line) are shown. Please note the different scales.

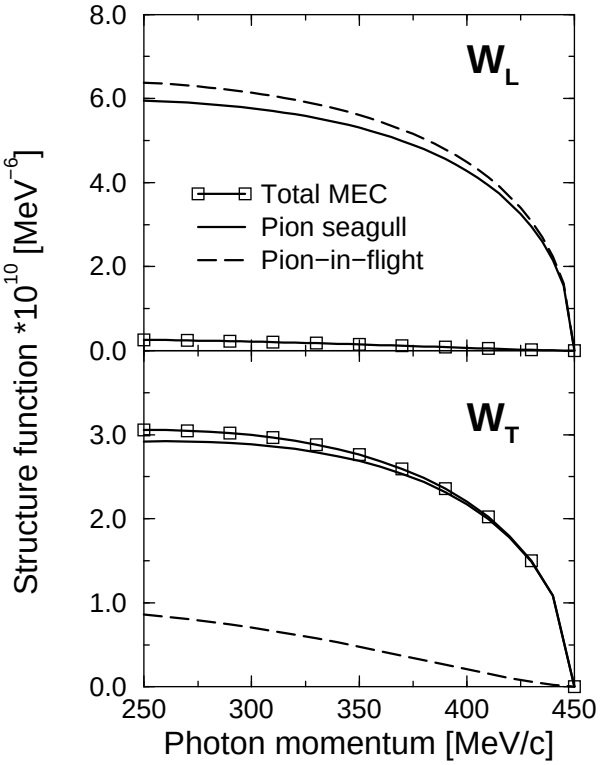

FIG. 6. MEC contribution for the asymmetric kinematical situation of Figure 5 (right part). The total MEC contribution (solid line with squares) consists of the π-seagull (solid line) and the π-in-flight contribution (dashed line).

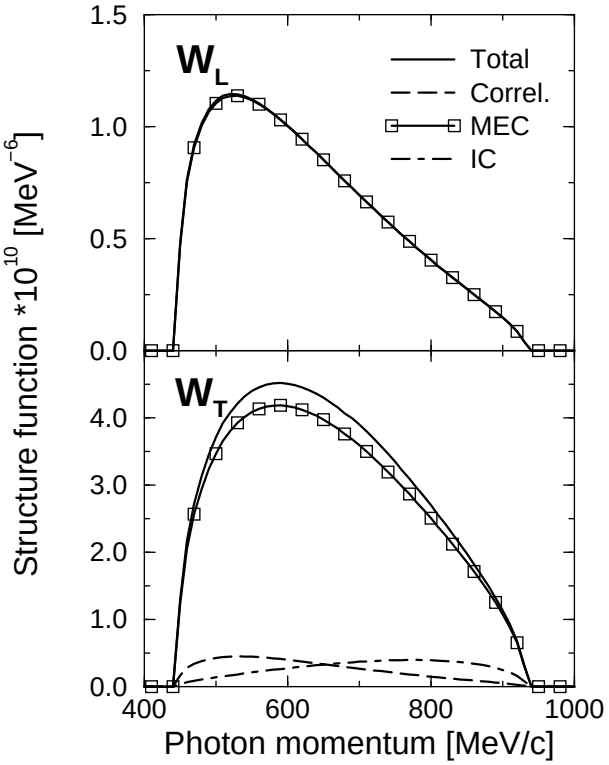

FIG. 7. Longitudinal (above) and transverse structure functions (below) for the knockout of a proton-neutron pair. The angles of the outgoing nucleons are $\theta'_p = \theta'_n = 30^\circ$ while the final kinetic energies are $T_p = T_n = 70\,\mathrm{MeV}$. The photon energy was chosen to be $\omega = 230\,\mathrm{MeV}$. The total structure functions (solid line) consist of the one-body current (dashed line), the MEC contribution (solid line with squares) and the IC contribution (dot-dashed line).

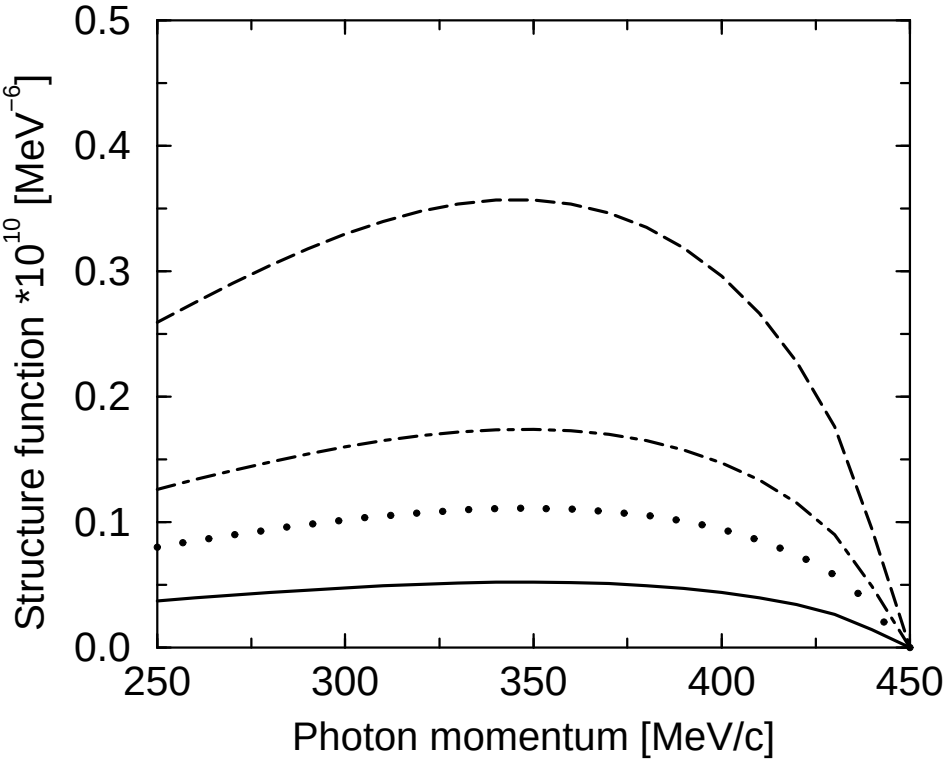

FIG. 8. The influence of the choice of the Δ propagator on the magnitude of the isobaric current contribution. Referring to the kinematical situation of Figure 5, matrix elements squared for different Δ propagators are shown. The solid line represents the propagator used in our calculations (c.f. eq. 17). A propagator of the form (19) for both resonant and non-resonant cases yields the dashed line, whereas the reduction to the static propagator (20) for the non-resonant case leads to the dot-dashed line. Finally, a propagator of the form suggested in [24] is reflected by the dotted curve. For further details, please refer to section II.C and the numerical results section.